Published in final edited form as:
Br J Nutr. 2012 February ; 107(4): 473–484. doi:10.1017/S0007114511003308.

Benefits of whole ginger extract in prostate cancer

Prasanthi Karna[1], **Sharmeen Chagani**[1], **Sushma R. Gundala**[1], **Padmashree C. G. Rida**[1], **Ghazia Asif**[1], **Vibhuti Sharma**[1], **Meenakshi V. Gupta**[2], and **Ritu Aneja**[1,*]

[1]Department of Biology, Georgia State University, Atlanta, GA 30303, USA

[2]West Georgia Hospitals, LaGrange, GA 30240, USA

Abstract

It is appreciated far and wide that increased and regular consumption of fruits and vegetables is linked with noteworthy anticancer benefits. Extensively consumed as a spice in foods and beverages worldwide, ginger (*Zingiber officinale* Roscoe) is an excellent source of several bioactive phenolics, including non-volatile pungent compounds such as gingerols, paradols, shogaols and gingerones. Ginger has been known to display anti-inflammatory, antioxidant and antiproliferative activities, indicating its promising role as a chemopreventive agent. Here, we show that whole ginger extract (GE) exerts significant growth-inhibitory and death-inductory effects in a spectrum of prostate cancer cells. Comprehensive studies have confirmed that GE perturbed cell-cycle progression, impaired reproductive capacity, modulated cell-cycle and apoptosis regulatory molecules and induced a caspase-driven, mitochondrially mediated apoptosis in human prostate cancer cells. Remarkably, daily oral feeding of 100 mg/kg body weight of GE inhibited growth and progression of PC-3 xenografts by approximately 56 % in nude mice, as shown by measurements of tumour volume. Tumour tissue from GE-treated mice showed reduced proliferation index and widespread apoptosis compared with controls, as determined by immunoblotting and immunohistochemical methods. Most importantly, GE did not exert any detectable toxicity in normal, rapidly dividing tissues such as gut and bone marrow. To the best of our knowledge, this is the first report to demonstrate the *in vitro* and *in vivo* anticancer activity of whole GE for the management of prostate cancer.

Keywords

Ginger extract; Prostate cancer; Apoptosis; Cell cycle; Chemoprevention

Prostate cancer is the most common non-cutaneous malignancy in American men, afflicting one in six men. It is estimated that in the USA, one new case occurs every 2·4 min and a death results every 16·4 min from prostate cancer. Clinically significant prostate cancer appears to develop over 20–30 years, thus presenting a ‘large window’ of opportunity for interventional chemopreventive strategies[1,2]. Although the traditional focus has been on treating existing tumours with chemotherapeutic agents that most often exert toxic side effects, development of chemopreventive approaches that can prevent, suppress or reverse progression to invasive cancer represents a relatively young field with tremendous promise to reduce cancer burden[3,4].

*Corresponding author: R. Aneja, fax +1 404 413 5301, raneja@gsu.edu.

The authors declare that they have no conflict of interest.

Laboratory and epidemiological research during the past three decades has provided indisputable evidence, indicating that high intake of fruits and vegetables is linked to a reduced cancer susceptibility including prostate cancer risk[5 – 7]. Several National Cancer Institute (NCI) initiatives continue to underscore the importance of including fruits and vegetables in the daily diet as a cancer chemopreventive measure[5,8 – 10]. Fruits and vegetables contain phytochemicals (carotenoids, polyphenolics, anthocyanins, alkaloids, N and S compounds) that have been shown to target multiple neoplastic stages to reduce overall cancer risk[11]. About thirty-five plant-based foods identified by the NCI to be effective in cancer prevention include garlic, ginger, turmeric, cruciferous vegetables (broccoli, brussel sprouts, cabbage) and grape seed extracts[12].

Ginger (*Zingiber officinale* Roscoe), a rhizomatous perennial plant used worldwide as a spice in foods and beverages, is commonly known for its medicinal properties, primarily as a remedy for digestive disorders, including dyspepsia, colic, nausea, vomiting, gastritis and diarrhoea[13]. Ginger is known to contain several bioactive phenolic compounds, including non-volatile pungent compounds such as gingerols, paradols, shogaols and gingerones[14]. The most abundant phytochemicals, gingerols, vary in chain length and comprise odiferous components of the fresh root, with 6-gingerol being the most imperative one[13]. The dehydrated form of gingerols, shogaols, mainly occurs in the dried roots, with 6-shogaol being the most abundant one[13]. The constituent phenolics of ginger have been shown to display antioxidant[15], anticancer[16], anti-inflammatory[17], anti-angiogenesis[18,19] and anti-artherosclerotic[20] properties.

Although the constituent phytochemicals present in ginger, in particular, gingerols, shogaols and paradols, are being rigorously tested for their anticancer properties, it is becoming increasingly recognisable that the gainful effects of fruits and vegetables are due to an additive and/or synergistic interplay of the composite mixture of phytochemicals present in whole foods rather than the constituent single agents alone[21]. In the context of ginger root, sufficient evidence suggests that achievable plasma concentrations of individual phytochemicals are in a very low micromolar range (2 μg/ml or less)[13]. In addition, these phytochemicals are found primarily in the form of their non-active glucuronide or sulphate metabolites, and therefore the anticancer effects observed with much higher concentrations *in vitro* may not be relevant in the *in vivo* milieu[22,23]. Thus, sufficient accumulating evidence suggests that the repertoire of phytochemicals present in dietary agents works together through complementary and overlapping mechanisms to present optimal cancer chemopreventive and therapeutic benefits[24]. With this mind-set, we sought to undertake a detailed evaluation of the *in vitro* and *in vivo* anticancer activity of whole ginger extract (GE) in prostate cancer. To the best of our knowledge, there is not even a single report that presents a thorough mechanistic investigation to develop GE for prostate cancer management.

Herein, we examined the *in vitro* and *in vivo* anticancer effects of GE in prostate cancer by evaluating its effects on cellular proliferation, cell-cycle progression and apoptosis. We found that GE resulted in growth inhibition, cell-cycle arrest and induced caspase-dependent intrinsic apoptosis in prostate cancer cells. *In vivo* studies suggested that GE significantly inhibited tumour growth in human PC-3 xenografts implanted in nude mice without any detectable toxicity.

Materials and methods

Preparation of ginger extract

Ginger was obtained from the local farmer’s market and extracts were prepared by soaking grated ginger in methanol overnight for four consecutive days. The supernatant was

collected daily and was finally concentrated *in vacuo* (Buchi Rotavap, Buchi, Switzerland), followed by freeze-drying using a lyophiliser to a solid powder form. GE stock solution was prepared by dissolving 100 mg/ml of dimethyl sulfoxide, and various concentrations were obtained by appropriate dilutions. The entire study was conducted using a single batch of GE to avoid batch-to-batch variation and maximise the product constancy.

Cell lines, media, antibody and reagents

Normal prostate epithelial cells (PrEC) and prostate cancer (LNCaP, C4-2, C4-2B, DU145 and PC-3), breast (MDA-MB-231 and MCF-7) and cervical (HeLa) cancer cell lines were used in the present study. The medium used to culture these cells was Roswell Park Memorial Institute-1640 (RPMI-1640) or Dulbecco's modified Eagle's medium supplemented with 10 % fetal bovine serum and 1 % antibiotic (penicillin/streptomycin). Primary antibodies to p21, cyclin E and BAX and horseradish peroxidase-conjugated secondary antibodies were from Santa Cruz Biotechnology (Santa Cruz, CA, USA). Cyclin D1, cdk4, p-Rb, Bcl2, cytochrome *c*, cleaved caspase-3 and cleaved poly (ADP-ribose)polymerase (PARP) were from Cell Signaling (Beverly, MA, USA), Ki67 was from Zymed (South San Francisco, CA, USA) and β-actin was from Sigma (St Louis, MO, USA).

In vitro proliferation and colony survival assay

Cells were plated in ninety-six-well plates and treated with gradient concentrations (1–1000 μg/ml) of GE the next day. After 72 h of incubation, cell proliferation was determined using the Alamar blue cell proliferation assay. The magnitude of the fluorescent signal is proportional to the number of live cells, and is monitored using 530–560 nm excitation wavelength and 590 nm emission[25] wavelength. For the colony assay, PC-3 cells were treated with 250 μg/ml of GE for 48 h, washed and replaced with regular RPMI medium. After 10 d, colonies were fixed with 4 % formaldehyde, stained with crystal violet and counted.

Cell-cycle progression studies by flow cytometry

For cell-cycle analysis, PC-3 cells were treated with vehicle (dimethyl sulfoxide) or GE at various doses (50, 100, 250, 500 and 1000 μg/ml) for 24 h or at a fixed dose of 250 μg/ml for various time points (12, 24, 48 and 72 h). At the end of incubation, cells were fixed with 70 % ethanol overnight, stained with propidium iodide containing RNase A, followed by data acquisition on a FACSCalibur flow cytometer (BD Biosciences, San Jose, CA, USA) and analyses using Flo-Jo software (Ashland, OR, USA).

Immunoblot analysis

Western blots were performed as described earlier[26]. Briefly, proteins were resolved by polyacrylamide gel electrophoresis and transferred onto polyvinylidene difluoride membranes (Millipore, Billerica, MA, USA). The membranes were blocked in Tris-buffered saline containing 0·05 % Tween-20 and 5 % fat-free dry milk and incubated first with primary antibodies and then with horseradish peroxidase-conjugated secondary antibodies. Specific proteins were visualised with enhanced chemiluminescence detection reagent according to the manufacturer's instructions (Pierce Biotechnology, Rockford, IL, USA).

Mitochondrial and cytosolic fractionation

To determine the release of cytochrome *c* from the mitochondria to the cytosol by immunoblotting, control or GE-treated (250 μg/ml) PC-3 cells were incubated on ice for 5 min in 100 μl of ice-cold cell lysis and mitochondria intact buffer (250 mM-sucrose, 70 mM-KCl and 100 μg digitonin/ml in PBS). The cells were pelleted and the supernatant containing cytosolic protein was stored at −80°C. The pellets were incubated at 4°C for 10

min in immunoprecipitation buffer (50 mM-Tris-HCl (pH 7·4), 150 mM-NaCl, 2 mM-EDTA, 2 mM-ethylene glycol tetra-acetic acid, 0·2 % Triton X-100, 0·3 % Nonidet P-40, 1 × Complete protease inhibitor; Roche Diagnostics Corporation, Indianapolis, IN, USA). The samples were centrifuged at high speed for 10 min at 4°C, and the supernatant containing mitochondrial protein was stored at −80°C[27]. Proteins were subjected to immunoblot analysis as described above.

Immunofluorescence microscopy

After treatment with 250 μg/ml of GE, PC-3 cells taken on glass coverslips were fixed with ice-cold methanol, followed by blocking with 2 % bovine serum albumin in PBS. Ki67, cleaved caspase-3 and PARP antibodies (1:250 dilution) were incubated with coverslips for 2 h at 37°C. The cells were washed with 2 % bovine serum albumin/PBS for 10 min at room temperature before incubating with a 1:500 dilution of Alexa 488- or Alexa 555-conjugated secondary antibodies. Cells were mounted with Prolong Gold antifade reagent that contains 4,6-diamidino-2-phenylindole (Invitrogen, Carlsbad, CA, USA).

JC-1 staining for mitochondrial transmembrane potential

Control and 250 μg/ml of GE-treated cells were labelled with JC-1 reagent for 15 min at 37°C. After washing, cell fluorescence was measured on a flow cytometer using orange–red emission filters.

Caspase-3/7 activity assay

Control or 250 μg/ml of GE-treated lysates were tested for caspase-3-like activity using Ac-DEVD-7-amino-4-trifluoromethyl-coumarin, which detects the activities of caspase-3 and caspase-7 according to the manufacturer's protocol (Calbiochem, San Diego, CA, USA). The results were evaluated using a fluorescence microplate reader and are expressed as relative fluorescence units.

In vivo tumour growth and treatment

Male Balb/c nude mice (6 weeks old) were obtained from the NCI (Frederick, MD, USA), and 10^6 PC-3 cells in 100 μl PBS were injected subcutaneously in the right flank without any basement membrane extracts such as Matrigel. The animals were given autoclave-sterilised standard diet pellets and water *ad libitum*. When tumours were palpable, mice were randomly divided into two groups. From each group, six mice were housed individually in one cage. The control group received vehicle and the treatment group received 100 mg/kg body weight of GE daily by oral administration. Tumour growth was monitored weekly using a vernier caliper and body weight was also recorded. All animal experiments were performed in compliance with the Institutional Animal Care and Use Committee (IACUC) guidelines.

Histopathological and immunohistochemical staining

After 8 weeks of vehicle or 100 mg/kg GE treatment, tumour, lung, spleen, adrenal, liver, gut, brain, kidney, heart, testes and bone marrow were formalin-fixed, paraffin-embedded and 5 μm thick sections were stained with Ki67, cleaved caspase-3, PARP and haematoxylin and eosin. Terminal deoxynucleotidyl transferase dUTP nick-end labelling (TUNEL) staining of tumour tissue sections was performed using the DeadEnd Fluorometric TUNEL System (Promega Inc., Madison, WI, USA) according to the manufacturer's instructions.

Statistical analysis

All the experiments were repeated at least three times. Results are expressed as mean values of at least three independent experiments and standard deviations, and *P* values (Student's *t* test) were calculated in reference to control values using Excel software.

Results

Ginger extract displays selective antiproliferative activity in prostate cancer cells

Although the whole GE has been shown to inhibit proliferation of breast[28] and colon cancer cells[29], there are no available reports that have tested the potential usefulness of GE in prostate cancer. Thus, we first asked whether GE affected the proliferation of prostate cancer cells. To this end, we investigated the effect of GE on PC-3, LNCaP, C4-2, C4-2B and DU145 cells, which are well-characterised representatives of androgen-responsive (LNCaP) and androgen-independent (PC-3, C4-2 and C4-2B) human prostate cancers. Cells were treated with increasing gradient concentrations of GE or vehicle (0·1 % dimethyl sulfoxide) for 72 h, and cell survival was assessed by the Alamar blue assay. Our data showed that GE inhibited cellular proliferation of all prostate cancer cells, with a half-maximal concentration of growth inhibition (IC_{50}) in the order C4-2 (512 μg/ml) > PC-3 (250 μg/ml) > C42-B (240 μg/ml) > DU145 (95 μg/ml) > LNCaP (75 μg/ml) (Fig. 1(A) and 1(B)). These data suggested the generality of the growth inhibition effect of GE on prostate cell lines with varying genotypic backgrounds. Hereupon, we focused on PC-3 cells for further experimentation to delineate molecular mechanisms of growth inhibition and cell death. We also performed a complementary trypan blue assay to examine cell viability on GE treatment in a concentration-and time-dependent manner in PC-3 cells (see Fig. S1 of the supplementary material, available online at http://www.journals.cambridge.org/bjn). Yet another screen of an array of cancer cell lines from different tissue types, namely breast and cervical cancer, showed that GE affected the proliferative capacity of these cancer cells (see Fig. S2 of the supplementary material, available online at http://www.journals.cambridge.org/bjn), suggesting generalisation of GE effects on cell lines from other tissue types.

Tumour cell selectivity is a highly desirable trait of any chemopreventive or chemotherapeutic regimen. To investigate whether GE-mediated suppression of PC-3 cell growth was selective to cancer cells, we determined the effect of GE treatment on a normal PrEC and serum-starved human dermal primary fibroblast (HDF) cells. Our choice of cell lines was based on the fact that PrEC and HDF exhibit features most consistent with the epithelial cells of prostate and dermal origin, respectively. The present results showed that the viability of PrEC or HDF was not significantly affected by GE treatment at concentrations in the range of 100–750 μg/ml (Fig. 1(B)). The IC_{50} of PrEC (1750 μg/ml) and HDF (1000 μg/ml) was approximately 6·9- and approximately 4-fold higher, respectively, compared with PC-3 cells, reflecting the wide therapeutic window that imparts tumour selectivity. Collectively, these results indicated that PC-3 cells, but not normal prostate epithelial or primary fibroblast cells, were significantly sensitive to growth inhibition by GE treatment.

Next, we performed a clonogenic cell survival assay to determine the ability of cells to proliferate indefinitely upon drug removal, thereby measuring their reproductive capacity to form colonies. Our data showed that 250 μg/ml of GE decreased colony numbers by approximately 66 % (Fig. 1(C)) compared with vehicle-treated controls. Representative pictures of surviving crystal violet-stained PC-3 cell colonies from control and GE-treated cells are shown in Fig. 1(C).

Several model systems have shown that Ki67 expression shows a good direct relationship with growth fraction, and thus serves as a reliable method for evaluating actively proliferating cell populations. Immunostaining with an antibody that reacts with the Ki67 nuclear antigen showed significantly intense staining in control cells compared with 250 μg/ml of GE-treated cells (Fig. 1(Di)). Fig. 1(Diii) is a bar graph representation of Ki67-positive cells scored as an average in both control and GE-treated samples from at least ten fields of vision totalling 200 cells. These data correlated with our previous *in vitro* proliferation and colony survival data, thus confirming the antiproliferative activity of GE.

Several characteristics of apoptosis, such as morphological and cellular changes, including chromatin condensation, membrane blebbing and DNA fragmentation, lend themselves to assessment. Thus, we microscopically examined DAPI-stained control and 48 h GE-treated (250 μg/ml) cells to observe condensed chromatin material and other morphological features reminiscent of apoptosis. Representative fluorescence micrographs are shown in Fig. 1(Dii) and their bar graph quantification is depicted in Fig. 1(Diii).

Ginger extract arrests cell-cycle progression at the G1 and S phase, followed by emergence of sub-G1 population

Several dietary agents have been shown to arrest the cell cycle, leading to growth inhibition and apoptosis. For example, grape seed proanthocyanidins, green tea polyphenols, epigallocatechin-3-gallate, resveratrol (red grapes, peanuts and berries), silymarin/silibinin (milk thistle), genistein (soyabean), curcumin (turmeric) and ginger (gingerols) affect cell-cycle progression at various stages by specifically modulating cell-cycle-associated proteins[30,31]. Specific gingerols, such as 6-gingerol and 8-gingerol, have been shown to perturb cell-cycle progression as a chemopreventive strategy[32]. Thus, our next aim was to gain mechanistic insights into GE-mediated antiproliferative activity by determining the specific cell-cycle stage at which GE intervenes. To this end, we examined the cell-cycle distribution profile of GE-treated PC-3 cells by employing a flow cytometric assay using the DNA intercalator dye, propidium iodide. Fig. 2(A) shows the effect of varying GE dose levels on cell-cycle progression of PC-3 cells at 24 h of treatment in a three-dimensional disposition. As shown in Fig. S3(A) of the supplementary material (available online at http://www.journals.cambridge.org/bjn), exposure of PC-3 cultures consistently resulted in a statistically significant dose-dependent enrichment of the sub-G1 fraction, suggesting considerable apoptotic cell death. The sub-G1 population increased from approximately 6 % at 100 μg/ml to approximately 99 % at 1000 μg/ml. Fig. S3(A) of the supplementary material (available online at http://www.journals.cambridge.org/bjn) bar-graphically depicts the percentages of G1, S, G2/M and sub-G1 phase populations in PC-3 cells upon treatment with varying GE doses (0–1000 μg/ml).

Next, we used the half-maximal sub-G1 dose (250 μg/ml) to explore in depth the effect of GE on each cell-cycle phase at the time of treatment (Fig. 2(B)). The present results showed that GE at a dose level of 250 μg/ml caused accumulation of cells in the G1 and S phase at as early as 6- and 12 h of GE treatment, respectively. The cell-cycle arrest was followed by an emergence of a hypodiploid sub-G1 population, a hallmark of dying apoptotic cells. The cell-cycle kinetics, as evident by the percentage of cells in various cell-cycle phases over time, is depicted in the form of a bar graph in Fig. S3(B) of the supplementary material (available online at http://www.journals.cambridge.org/bjn). The sub-G1 population began to appear at as early as 6 h and peaked at 48 h (approximately 67 %).

To further understand the interrelationships between the effect of GE on cell-cycle arrest and induction of apoptosis, we devised timed exposure experiments using two regimens. The first regimen involved low GE concentration (50 μg/ml) for a longer time (72 h), whereas the second regimen was exposure to a higher GE dose (1000 μg/ml) for a shorter duration (6

h). Essentially, the idea was to delineate whether either treatment regimen caused cell-cycle arrest and/or apoptosis simultaneously or sequentially. The present results indicated that short-term exposure of higher concentration induced considerable cell death (approximately 35 %) without any apparent cell-cycle arrest, whereas long-term exposure to a lower dose induced cell-cycle arrest (G2/M) and significant cell death or apoptosis (approximately 50 %; see Fig. S4 of the supplementary material, available online at http://www.journals.cambridge.org/bjn). This suggested that long-term exposure (72 h) to low-dose (50 μg/ml) GE induced cell-cycle arrest, which perhaps lends sufficient time for enhanced expression of pro-apoptotic molecules that ultimately results in a higher proportion of sub-G1 cells (50 %), indicative of apoptosis.

Taken together, these observations imply that the growth inhibition of PC-3 cells by GE results from a combination of apoptosis and cell-cycle derangements, in which cell-cycle arrest may be a key event. The simultaneous appearance of cell-cycle arrest and apoptosis at a low dose for a longer time perhaps suggests that cell death may be ascribed to the activation of apoptotic pathways as a consequence of the inability of the cells to overcome growth arrest and proceed through the cell cycle. Nonetheless, on the basis of the appearance of sub-G1 cells at 6 h after treatment with 1000 μg/ml of GE, we cannot exclude the possibility that cell death may be a primary direct effect of GE. It is also likely that other non-apoptotic means of cell death at either treatment regimen might exist. However, the end result of both perturbations (low-dose, long-term and high-dose, short-term) is induction of PC-3 cell death. These data suggest that GE could potentially be tested as a potential chemopreventive as well as a chemotherapeutic agent for prostate cancer management.

Effect of ginger extract treatment on cell-cycle and apoptosis regulatory molecules

We next sought to determine molecular mechanisms underlying GE-induced cell-cycle stasis and subsequent apoptosis. Essentially, cell-cycle progression involves sequential activation of cdks by their cyclical association with cell-cycle phase-specific regulatory cyclin molecules[33]. To examine GE-induced alterations, we first determined the effect of 250 μg/ml of GE on protein levels of G1/S-specific cyclins and cdks by immunoblotting methods. GE treatment caused a marked decrease in cyclin D1 levels in PC-3 cells, which was evident as early as 12 h post-treatment (Fig. 2(C)). In addition, GE-treated PC-3 cells exhibited a slight decrease in cdk4 levels (Fig. 2(C)). Our data also showed that GE caused a significant reduction in cyclin E levels, which drive the cell cycle primarily through the S phase in association with cdk2.

Elevated levels of p21, a cdk inhibitor, function to stall the cell cycle[34]. Essentially, p21 plays a crucial role in the regulation of the G1/S and G2/M transition by binding to and inhibiting the kinase activity of cyclin/cdk complexes. To explore further, we determined the effect of GE treatment on protein expression and/or phosphorylation of p21 and Rb by immunoblotting methods. As shown in Fig. 2(C), GE treatment caused an induction of p21 protein expression in PC-3 cells, which was evident at 12–24 h. In addition, GE treatment caused suppression of Rb phosphorylation in PC-3 cells (Fig. 2(C)).

Effect of ginger extract treatment on Bcl-2 family members

Multiple apoptotic pathways are recruited by cells for executing their own demise via apoptosis. Among them, one major mechanism involves the loss of mitochondrial membrane integrity and transmembrane potential (Ψm)[35]. We thus asked whether GE affected mitochondrial transmembrane potential. To this end, we stained GE-treated cells with JC-1, a cationic dye that displays potential-dependent accumulation in the mitochondria. A decrease in the red:green fluorescence intensity ratio suggested mitochondrial depolarisation (Fig. 2(Di)). The increase in the green JC-1 monomeric form, indicative of collapse of

transmembrane potential, was quantitatively determined using flow cytometry. Quantification of fluorescence-activated cell sorting data indicated an approximately 3·6-fold increase (Fig. 2(Dii)) in the mean fluorescence intensity of GE-treated JC-1-stained cells compared with controls (Fig. 2(Dii)). A spectral shift and loss of red fluorescence, which is consistent with decreased polarisation, was also observed (Fig. 2(Ei) and (Eii)). The collapse of Ψm is closely associated with alterations in the ratio of anti-apoptotic:pro-apoptotic members of the Bcl2 family, which determines susceptibility to apoptosis[36]. Particularly, loss of Ψm is coupled with hyperphosphorylation and thus inactivation of the anti-apoptotic molecule Bcl2, which promotes recruitment of BAX onto the outer mitochondrial membrane. BAX incorporation results in uncoupling of the respiratory chain and efflux of small pro-apoptotic factors, such as cytochrome *c*, leading to the activation of key executioner caspases, caspase-3/7. Thus, our next step was to investigate the effect of GE treatment on levels of Bcl-2 family proteins by immunoblotting and the results are shown in Fig. 3(A). GE treatment caused a rapid and marked increase in BAX expression over time, whereas levels of total Bcl2 were decreased (Fig. 3(A)). The GE-mediated alterations in the pro-apoptotic/anti-apoptotic molecules were evident as early as 12 h post-treatment and increased thereafter (Fig. 3(A)). Biochemical events, such as the release of cytochrome *c* from the mitochondria into the cytosol, caspase activation and PARP cleavage, predominantly occur during mitochondria-mediated apoptotic cell death. Thus, we asked whether GE-induced cell death promoted the release of apoptogenic factors from the mitochondria that triggered the downstream executioner events of apoptosis. Our data showed that cytochrome *c* was detectable at 12 h and peaked at 48 h of GE treatment in the cytosolic fraction, as observed using immunoblotting methods (Fig. 3(A)). Immunofluorescence microscopic methods also showed translocation of cytochrome *c* into the cytosol at 24 h of GE treatment (see Fig. S5 of the supplementary material, available online at http://www.journals.cambridge.org/bjn).

Activation of executioner caspase-3 and cleavage of poly(ADP-ribose)polymerase

Our next aim was to explore the involvement of caspases that are activated by the release of cytochrome *c* and are known to cleave a variety of substrates. Since caspase-3 activation is considered as a hallmark of apoptosis, we monitored the active form of the cysteine protease using a small, conserved, modified peptide substrate that becomes fluorogenic upon cleavage. As shown in Fig. 3(B), GE stimulated a time-dependent increase of caspase-3 activity in PC-3 cells. However, treatment of cells with a specific inhibitor of caspase-3 significantly blocked GE-induced apoptotic cell death (data not shown). Furthermore, immunoblots showed a time-dependent increase in expression levels of activated caspase-3, suggesting that GE-induced cell death is caspase-3 dependent (Fig. 3(A)). On caspase-3 activation, a number of cellular proteins are cleaved, including PARP. The present results showed a time-dependent increase in cleaved PARP levels, a substrate of caspase-3. An increase in the expression of both activated caspase-3 and cleaved PARP was also confirmed in GE-treated cells by immunofluorescence microscopic methods (Fig. 3(Ci) and (Di)). Quantification was performed by scoring positive cells in control and GE-treated PC-3 cells from several random image fields totalling 200 cells (Fig. 3(Cii) and (Dii)).

We also examined the ability of GE to induce apoptosis in androgen-responsive LNCaP cells, and our data showed a dose-dependent increase in the sub-G1 population evaluated at 24 h of GE treatment (Fig. S6(A)). There was also an increase in cleaved caspase-3 levels and caspase-3 activity, as shown in Fig. S6(B) and (C) of the supplementary material (available online at http://www.journals.cambridge.org/bjn).

Oral ginger extract feeding achieves inhibition of PC-3 tumours in nude mice

Having identified significant antiproliferative and pro-apoptotic activity of GE, an intriguing question was to determine whether the anticancer effects of GE were restricted to *in vitro* cultures or extended to *in vivo* systems. To validate this, we examined the efficacy of GE to inhibit human prostate PC-3 xenografts subcutaneously implanted in athymic nude mice. Animals in the treatment group were fed daily with 100 mg/kg GE. The GE was dissolved in PBS containing 0·5 % Tween-80 and was fed by oral administration for 8 weeks; responses to GE treatment were followed by tumour volume measurements every consecutive day using vernier calipers (Fig. 4(A)). Tumours in vehicle-treated control animals showed unrestricted progression (Fig. 4(A)), whereas GE feeding showed a time-dependent inhibition of tumour growth over 8 weeks (Fig. 4(A)). A reduction in tumour burden by approximately 56 % was observable after 8 weeks of 100 mg/kg per d oral feeding, and the difference between the mean final tumour volumes in animals receiving GE and those receiving vehicle orally was statistically significant ($P<0·05$). All animals in the control group were euthanised by day 60 post-inoculation, in compliance with the IACUC guidelines. To assess the overall general health and well-being of animals during GE treatment, body weights were recorded twice a week. GE-treatment was well tolerated, and mice maintained normal weight gain (Fig. 4(B)) and showed no signs of discomfort during the treatment regimen. At the end point of the animal experiments (week 8), the excised tumours were weighed and an approximately 53 % reduction in tumour weight was observed in the GE-treated group compared with controls (see Fig. S7 of the supplementary material, available online at http://www.journals.cambridge.org/bjn).

In vivo mechanisms of ginger extract-mediated inhibition of tumour growth

To investigate the *in vivo* mechanisms of tumour inhibition, we first examined haematoxylin- and eosin-stained tumour sections from control and GE-treated mice. Tumour microsections from GE-treated mice showed large areas of tumour cell death, seen as tumour necrosis adjacent to normal-looking healthy cells. Significant loss of tumorigenic cells in GE-treated animals (Fig. 4(C)) was consistent with the therapeutic effect of GE. However, some viable tumour cells were observed at the periphery of cell death zones. In contrast, microsections from control tumour tissues revealed sheets of tumour cells with high-grade pleomorphic nuclei (Fig. 4(C)).

We next evaluated the *in vivo* effect of GE feeding on the antiproliferative response associated with the inhibition of tumour growth. To this end, tumour tissue lysates were analysed for cyclins (D1, E and B1) and a cyclin-dependent kinase inhibitor, p21, using immunoblotting methods (Fig. 4(D)). GE treatment caused a decrease in cyclin D1, cyclin E and cyclin B1, whereas it increased p21 expression levels, which allied with the present *in vitro* findings in PC-3 cells (Fig. 2(C)). Alterations of these cell-cycle regulatory molecules in tumour tissue from GE-treated mice suggest a potential mechanism for inhibition of tumour proliferation, in keeping with the inhibition of cell-cycle kinetics observed *in vitro* (Fig. 2(A) and (B) and see Fig. S3(A) and (B) of the supplementary material, available online at http://www.journals.cambridge.org/bjn). *In vivo* apoptotic responses of GE feeding in mice bearing PC-3 tumour xenografts were evaluated by immunoblotting of tumour lysates for cleaved caspase-3 expression.

We further correlated the *in vivo* molecular mechanisms of GE treatment by immunostaining for Ki67, a marker for cell proliferation, as well as apoptotic markers such as cleaved caspase-3, cleaved PARP and TUNEL (Fig. 5(A)). Tumour samples from the treated groups receiving GE showed marked reduction in Ki67-positive cells compared with controls (Fig. 5(A)). There was a significantly higher expression of cleaved caspase-3 (approximately 12-fold) and PARP (approximately 35-fold) in tumour-tissue from the GE-

treated groups compared with controls (Fig. 5(A) and (B)). We found an approximately 18-fold increase in TUNEL-positive cells in GE-treated tumours compared with controls (Fig. 5(A) and (B)). Fig. 5(B) shows bar graph quantitative representation of the immunostaining data from the control and GE-treated groups.

Ginger extract treatment is non-toxic

Toxicity, particularly in tissues with actively proliferating cells, remains a major concern in the chemotherapy of prostate cancer patients. We observed that there was no gross toxicity, as measured in terms of body weight, grooming or lethargy in GE-treated mice. Our data showed that there were no detectable differences in the histological appearance of tissues, including in the gut, liver, spleen, lung, brain, heart, testes and bone marrow, from vehicle- and GE-treated tumour-bearing mice (see Fig. S8 of the supplementary material, available online at http://www.journals.cambridge.org/bjn). To determine whether GE treatment affected proliferation of normal tissues with rapidly proliferating cells, colonic crypts from GE-treated and vehicle-treated mice were stained with Ki67, a marker for proliferative index. We found that colonic crypts from both mice groups showed comparable nuclear Ki67 staining (see Fig. S9 of the supplementary material, available online at http://www.journals.cambridge.org/bjn). These data suggested that GE did not affect normal tissues with rapidly proliferating cells. In addition, serum biochemical markers (alanine transaminase, alkaline phosphatase, γ-glutamyl transpeptidase for hepatic function, and creatinine and electrolytes, e.g. K, Na, Ca and Cl, for renal function) were similar between the control and GE-treated groups (see Fig. S10 of the supplementary material, available online at http://www.journals.cambridge.org/bjn), indicating the absence of apparent toxicity.

Discussion

‘An ounce of prevention is worth a pound of cure’ goes the famous adage that holds true for cancer chemoprevention strategies using dietary agents such as fruits and vegetables. Phytochemical extracts from fruits and vegetables are increasingly being shown to exert potent antioxidant and antiproliferative effects[21]. It is widely becoming appreciated that chemopreventive agents offer superior potential in the long term than chemotherapeutic agents, as lifestyle and dietary habits have been identified as major risk factors, particularly in prostate cancer growth and progression[37,38].

Ginger rhizome is extensively used in the form of a fresh paste or dried powder to flavour food and beverages in places such as India and China[14]. The present study reports a novel finding that oral consumption of the extract of whole ginger, a commonly consumed vegetable worldwide, significantly inhibits prostate tumour progression in both *in vitro* and *in vivo* mice models. The anticancer effect of GE was coupled with its significant antiproliferative, cell-cycle inhibitory and pro-apoptotic activity in cell culture as well as in prostate tumour xenograft models. In addition, we also identified that GE strongly suppressed *in vitro* and *in vivo* expression of cyclins/cdks that intricately orchestrate cell-cycle progression.

Ginger is rich in both hydrophilic and hydrophobic constituents, with the hydrophobic portion mainly comprising different kinds of monoterpenes, oxygenated monoterpenes, sesquiterpenes, zingerone, paradols, gingerols and shogaols other than essential oils[39]. Shogaol is a dehydrated product of structurally similar gingerols[40]. Just as large quantity of gingerols is found in fresh ginger, shogaols are abundant in dried and thermally treated ginger[40]; on the other hand, the hydrophilic portion of GE mostly has a variety of polyphenolic compounds[41]. Quantitative reports have suggested that the main constituents such as 6-gingerol, 8-gingerol, 10-gingerol and 6-shogaol are present in GE to an extent of

2·15, 0·72, 1·78 and 0·37 %, respectively[13]. Recent studies have shown that 6-gingerol, the major pungent constituent of ginger, suppresses carcinogenesis in skin[19,42], gastrointestinal[43], colon[29] and breast[28]. The effective *in vitro* dose level for 6-gingerol in a variety of cancer cells has been reported to be in the range of 300–400 μM[32], which translates to 88–177 μg/ml. This is interesting as on the basis of our whole GE data (IC_{50} value = 250 μg/ml), IC_{50} for 6-gingerol computes to only 5·38 μg/ml (approximately 18 μM). These observations raise the possibility of the presence of more active ingredients or existence of an additive and/or synergistic relationship between the bioactive constituents in GE. Furthermore, pharmacokinetic studies have reported the maximum achievable plasma concentrations of 6-gingerol as 1·90 (SD 0·97) μg/ml (approximately 6·4 (SD 3·3) μM) on oral administration of 120 mg/kg of 6-gingerol in rats[44]. This suggests that the maximum levels of 6-gingerol achievable in the plasma are much lower compared with the reported *in vitro* effective half-maximal dose (300–400 μM), thus limiting its potential efficacy in humans. This notion is in agreement with accumulating data that suggest that the additive/synergistic effects of the constituent phytochemicals in fruits and vegetables are accountable for their potent anti-oxidant and anticancer activities[21]. This emerging paradigm is further supported by clinical trials with pure single phytochemicals such as α-tocopherol, β-carotene and vitamin C that have met with limited success[24,45,46], reinforcing the fact that an isolated single constituent of a complex mixture of phytochemicals present in foods may lose its bioactivity[21]. In the light of these arguments, the remarkable anticancer activity of whole GE, without any detectable toxicity in the present study, certainly underscores the importance of using whole food extracts. Essentially, the beneficial effects of constituent phytochemicals at much lower dose levels when present together compared with high, relatively toxic doses when used as single agents may be ascribable to complex inter-reactivity or interdependence existent among various constituent phytochemicals. This may also be attributable to the fact that the various phytochemicals comprising whole foods vary in their molecular size, hydrophilicity and solubility. Thus, there is a strong likelihood that a particular combination of phytochemicals perhaps offers the optimal pharmacokinetic and pharmacodynamic properties that dictate favourable anticancer responses. However, if the constituents that participate in the ‘optimal combination’ are singled out, it may result in altered bioavailability and distribution of the phytochemicals in different macromolecules, subcellular organelles, cells, organs and tissues to yield suboptimal or an absence of favourable therapeutic responses[24].

Given our anticancer therapeutic doses of GE in reducing tumour burden in mice bearing human prostate xenografts, we performed allometric scaling calculations to extrapolate the mice data to humans, and the human equivalent dose of the GE was found to be approximately 567 mg for a 70 kg adult[47], which perhaps can be obtained from about 100 g of fresh ginger. Although various other pharmacokinetic and pharmacodymanic factors need to be considered before any such conclusions on dose extrapolations can be drawn, our data present the potential usefulness of GE in prostate cancer and warrant further studies. In conclusion, the present study is the first report to describe identification and detailed evaluation of *in vitro* and *in vivo* anticancer activity of whole GE in the therapeutic management of human prostate cancer.

Supplementary Material

Refer to Web version on PubMed Central for supplementary material.

Acknowledgments

The present study was supported by grant to R. A. from the National Cancer Institute at the National Institutes of Health (NCI/NIH, 1R00CA131489). P. K. conducted most of the research and analysed the data, S. C. conducted

the animal experiments, V. S. made the GE and M. V. G. evaluated the pathology of normal tissues and tumour sections. G. A. and P. C. G. R. contributed to the editing of the manuscript. R. A. designed the research and wrote the manuscript. All authors read and approved the final manuscript. R. A. acknowledges financial support from the NCI/NIH.

Abbreviations

GE	ginger extract
HDF	human dermal primary fibroblast
IACUC	Institutional Animal Care and Use Committee
IC_{50}	half-maximal concentration of growth inhibition
NCI	National Cancer Institute
PARP	poly(ADP-ribose)polymerase
PrEC	prostate epithelial cell
RPMI-1640	Roswell Park Memorial Institute-1640
TUNEL	terminal deoxynucleotidyl transferase dUTP nick-end labelling

References

1. Syed DN, Khan N, Afaq F, et al. Chemoprevention of prostate cancer through dietary agents: progress and promise. Cancer Epidemiol Biomarkers Prev. 2007; 16:2193–2203. [PubMed: 18006906]
2. Nelson WG, De Marzo AM, Isaacs WB. Prostate cancer. N Engl J Med. 2003; 349:366–381. [PubMed: 12878745]
3. Sporn MB. Approaches to prevention of epithelial cancer during the preneoplastic period. Cancer Res. 1976; 36:2699–2702. [PubMed: 1277177]
4. Mann JR, Backlund MG, DuBois RN. Mechanisms of disease: inflammatory mediators and cancer prevention. Nat Clin Pract Oncol. 2005; 2:202–210. [PubMed: 16264935]
5. Kaur M, Agarwal C, Agarwal R. Anticancer and cancer chemopreventive potential of grape seed extract and other grape-based products. J Nutr. 2009; 139:1806S–1812S. [PubMed: 19640973]
6. Cooke D, Steward WP, Gescher AJ, et al. Anthocyans from fruits and vegetables – does bright colour signal cancer chemopreventive activity? Eur J Cancer. 2005; 41:1931–1940. [PubMed: 16084717]
7. Yang CS, Landau JM, Huang MT, et al. Inhibition of carcinogenesis by dietary polyphenolic compounds. Annu Rev Nutr. 2001; 21:381–406. [PubMed: 11375442]
8. Traka M, Gasper AV, Melchini A, et al. Broccoli consumption interacts with GSTM1 to perturb oncogenic signalling pathways in the prostate. PLoS One. 2008; 3:e2568. [PubMed: 18596959]
9. Steinkellner H, Rabot S, Freywald C, et al. Effects of cruciferous vegetables and their constituents on drug metabolizing enzymes involved in the bioactivation of DNA-reactive dietary carcinogens. Mutat Res. 2001:480–481. 285–297.
10. Colli JL, Amling CL. Chemoprevention of prostate cancer: what can be recommended to patients? Curr Urol Rep. 2009; 10:165–171. [PubMed: 19371472]
11. Craig WJ. Health-promoting properties of common herbs. Am J Clin Nutr. 1999; 70(Suppl 3): 491S–499S. [PubMed: 10479221]
12. Surh YJ. Cancer chemoprevention with dietary phytochemicals. Nat Rev Cancer. 2003; 3:768–780. [PubMed: 14570043]
13. Zick SM, Djuric Z, Ruffin MT, et al. Pharmacokinetics of 6-gingerol, 8-gingerol, 10-gingerol, and 6-shogaol and conjugate metabolites in healthy human subjects. Cancer Epidemiol Biomarkers Prev. 2008; 17:1930–1936. [PubMed: 18708382]

14. Shukla Y, Singh M. Cancer preventive properties of ginger: a brief review. Food Chem Toxicol. 2007; 45:683–690. [PubMed: 17175086]
15. Shobana S, Naidu KA. Antioxidant activity of selected Indian spices. Prostaglandins Leukot Essent Fatty Acids. 2000; 62:107–110. [PubMed: 10780875]
16. Katiyar SK, Agarwal R, Mukhtar H. Inhibition of tumor promotion in SENCAR mouse skin by ethanol extract of *Zingiber officinale* rhizome. Cancer Res. 1996; 56:1023–1030. [PubMed: 8640756]
17. Surh YJ. Anti-tumor promoting potential of selected spice ingredients with antioxidative and anti-inflammatory activities: a short review. Food Chem Toxicol. 2002; 40:1091–1097. [PubMed: 12067569]
18. Kim EC, Min JK, Kim TY, et al. [6]-Gingerol, a pungent ingredient of ginger, inhibits angiogenesis *in vitro* and *in vivo*. Biochem Biophys Res Commun. 2005; 335:300–308. [PubMed: 16081047]
19. Kim SO, Kundu JK, Shin YK, et al. [6]-Gingerol inhibits COX-2 expression by blocking the activation of p38 MAP kinase and NF-kappaB in phorbol ester-stimulated mouse skin. Oncogene. 2005; 24:2558–2567. [PubMed: 15735738]
20. Fuhrman B, Rosenblat M, Hayek T, et al. Ginger extract consumption reduces plasma cholesterol, inhibits LDL oxidation and attenuates development of atherosclerosis in atherosclerotic, apolipoprotein E-deficient mice. J Nutr. 2000; 130:1124–1131. [PubMed: 10801908]
21. Liu RH. Health benefits of fruit and vegetables are from additive and synergistic combinations of phytochemicals. Am J Clin Nutr. 2003; 78 (Suppl 3):517S–520S. [PubMed: 12936943]
22. Yang CS. Inhibition of carcinogenesis by tea. Nature. 1997; 389:134–135. [PubMed: 9296488]
23. Jankun J, Selman SH, Swiercz R, et al. Why drinking green tea could prevent cancer. Nature. 1997; 387:561. [PubMed: 9177339]
24. Liu RH. Potential synergy of phytochemicals in cancer prevention: mechanism of action. J Nutr. 2004; 134(Suppl 12):3479S–3485S. [PubMed: 15570057]
25. Nociari MM, Shalev A, Benias P, et al. A novel one-step, highly sensitive fluorometric assay to evaluate cell-mediated cytotoxicity. J Immunol Methods. 1998; 213:157–167. [PubMed: 9692848]
26. Karna P, Zughaier S, Pannu V, et al. Induction of reactive oxygen species-mediated autophagy by a novel microtubule-modulating agent. J Biol Chem. 2010; 285:18737–18748. [PubMed: 20404319]
27. Waterhouse NJ, Goldstein JC, von Ahsen O, et al. Cytochrome *c* maintains mitochondrial transmembrane potential and ATP generation after outer mitochondrial membrane permeabilization during the apoptotic process. J Cell Biol. 2001; 153:319–328. [PubMed: 11309413]
28. Lee HS, Seo EY, Kang NE, et al. [6]-Gingerol inhibits metastasis of MDA-MB-231 human breast cancer cells. J Nutr Biochem. 2008; 19:313–319. [PubMed: 17683926]
29. Jeong CH, Bode AM, Pugliese A, et al. [6]-Gingerol suppresses colon cancer growth by targeting leukotriene A4 hydrolase. Cancer Res. 2009; 69:5584–5591. [PubMed: 19531649]
30. Aggarwal BB, Shishodia S. Molecular targets of dietary agents for prevention and therapy of cancer. Biochem Pharmacol. 2006; 71:1397–1421. [PubMed: 16563357]
31. Meeran SM, Katiyar SK. Cell cycle control as a basis for cancer chemoprevention through dietary agents. Front Biosci. 2008; 13:2191–2202. [PubMed: 17981702]
32. Park YJ, Wen J, Bang S, et al. [6]-Gingerol induces cell cycle arrest and cell death of mutant p53-expressing pancreatic cancer cells. Yonsei Med J. 2006; 47:688–697. [PubMed: 17066513]
33. Grana X, Reddy EP. Cell cycle control in mammalian cells: role of cyclins, cyclin dependent kinases (CDKs), growth suppressor genes and cyclin-dependent kinase inhibitors (CKIs). Oncogene. 1995; 11:211–219. [PubMed: 7624138]
34. Besson A, Dowdy SF, Roberts JM. CDK inhibitors: cell cycle regulators and beyond. Dev Cell. 2008; 14:159–169. [PubMed: 18267085]
35. Green DR, Reed JC. Mitochondria and apoptosis. Science. 1998; 281:1309–1312. [PubMed: 9721092]

36. Adams JM, Cory S. The Bcl-2 protein family: arbiters of cell survival. Science. 1998; 281:1322–1326. [PubMed: 9735050]
37. Kelloff GJ, Sigman CC, Greenwald P. Cancer chemoprevention: progress and promise. Eur J Cancer. 1999; 35:2031–2038. [PubMed: 10711244]
38. Bidoli E, Talamini R, Bosetti C, et al. Macronutrients, fatty acids, cholesterol and prostate cancer risk. Ann Oncol. 2005; 16:152–157. [PubMed: 15598953]
39. Saha S, Smith RM, Lenz E, et al. Analysis of a ginger extract by high-performance liquid chromatography coupled to nuclear magnetic resonance spectroscopy using superheated deuterium oxide as the mobile phase. J Chromatogr A. 2003; 991:143–150. [PubMed: 12703908]
40. Jolad SD, Lantz RC, Solyom AM, et al. Fresh organically grown ginger (*Zingiber officinale*): composition and effects on LPS-induced PGE2 production. Phytochemistry. 2004; 65:1937–1954. [PubMed: 15280001]
41. Kato A, Higuchi Y, Goto H, et al. Inhibitory effects of *Zingiber officinale* Roscoe derived components on aldose reductase activity *in vitro* and *in vivo*. J Agric Food Chem. 2006; 54:6640–6644. [PubMed: 16939321]
42. Park KK, Chun KS, Lee JM, et al. Inhibitory effects of [6]-gingerol, a major pungent principle of ginger, on phorbol ester-induced inflammation, epidermal ornithine decarboxylase activity and skin tumor promotion in ICR mice. Cancer Lett. 1998; 129:139–144. [PubMed: 9719454]
43. Yoshimi N, Wang A, Morishita Y, et al. Modifying effects of fungal and herb metabolites on azoxymethane-induced intestinal carcinogenesis in rats. Jpn J Cancer Res. 1992; 83:1273–1278. [PubMed: 1483942]
44. Wang W, Li CY, Wen XD, et al. Plasma pharmacokinetics, tissue distribution and excretion study of 6-gingerol in rat by liquid chromatography–electrospray ionization time-of-flight mass spectrometry. J Pharm Biomed Anal. 2009; 49:1070–1074. [PubMed: 19217234]
45. The Alpha-Tocopherol, Beta Carotene Cancer Prevention Study Group. The effect of vitamin E and beta carotene on the incidence of lung cancer and other cancers in male smokers. N Engl J Med. 1994; 330:1029–1035. [PubMed: 8127329]
46. Omenn GS, Goodman GE, Thornquist MD, et al. Effects of a combination of beta carotene and vitamin A on lung cancer and cardiovascular disease. N Engl J Med. 1996; 334:1150–1155. [PubMed: 8602180]
47. Reagan-Shaw S, Nihal M, Ahmad N. Dose translation from animal to human studies revisited. FASEB J. 2008; 22:659–661. [PubMed: 17942826]

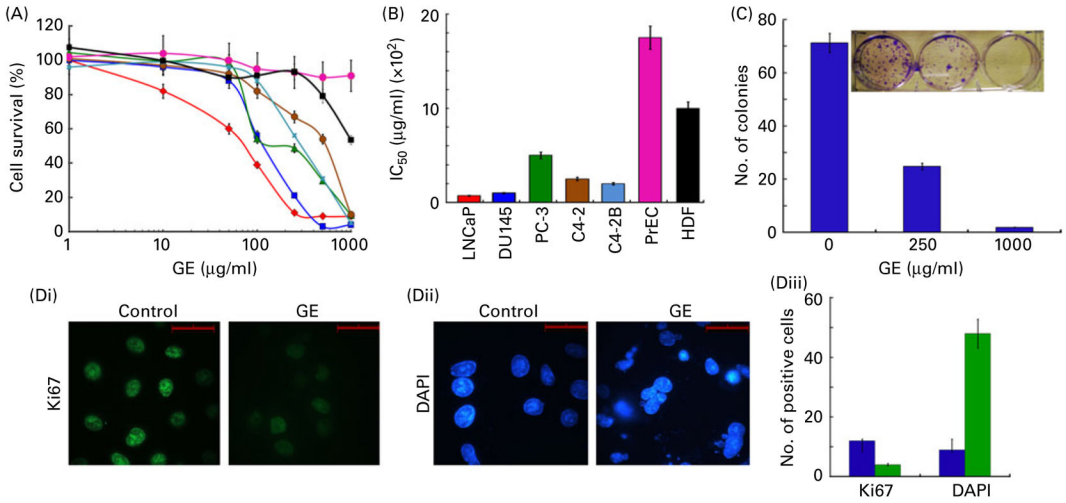

Fig. 1.

Ginger extract (GE) has potent antiproliferative activity. Human prostate cancer LNCaP ( ), DU145 ( ), PC-3 ( ), C4-2 ( ), C4-2B ( ) cells, as well as normal prostate epithelial cells (PrEC,) and human dermal primary fibroblasts (HDF,) were treated with gradient concentrations of GE for 72 h. The percentage of cell proliferation at indicated concentrations, compared with untreated control cells, was measured by the *in vitro* cell proliferation assay, as described in Materials and methods. (A) Plot of percentage of cell survival *vs.* GE concentrations used for the determination of half-maximal concentration of growth inhibition (IC_{50}) values. Values are means of three independent experiments performed in triplicate, with standard deviations represented by vertical bars ($P<0{\cdot}05$). (B) Bar graph representation of the IC_{50} of the indicated cell lines. (C) Bar graph representation and photograph of crystal violet-stained surviving colonies from the control and GE-treated (250 and 1000 μg/ml) groups. (D) Fluorescence micrographs of control and GE-treated PC-3 cells stained for (Di) Ki67 (green) or (Dii) 4′,6-diamidino-2-phenylindole (DAPI, blue). Scale bar, 20 μm. (Diii) Quantification of Ki67-postive or DAPI-stained cells in control ( ) and 250 μg/ml of GE-treated PC-3 cells ( ) from random image fields totalling 200 cells. Values are means, with standard deviations represented by vertical bars. Mean values were significantly different from the controls ($P<0{\cdot}05$). (A colour version of this figure can be found online at www.journals.cambridge.org/bjn).

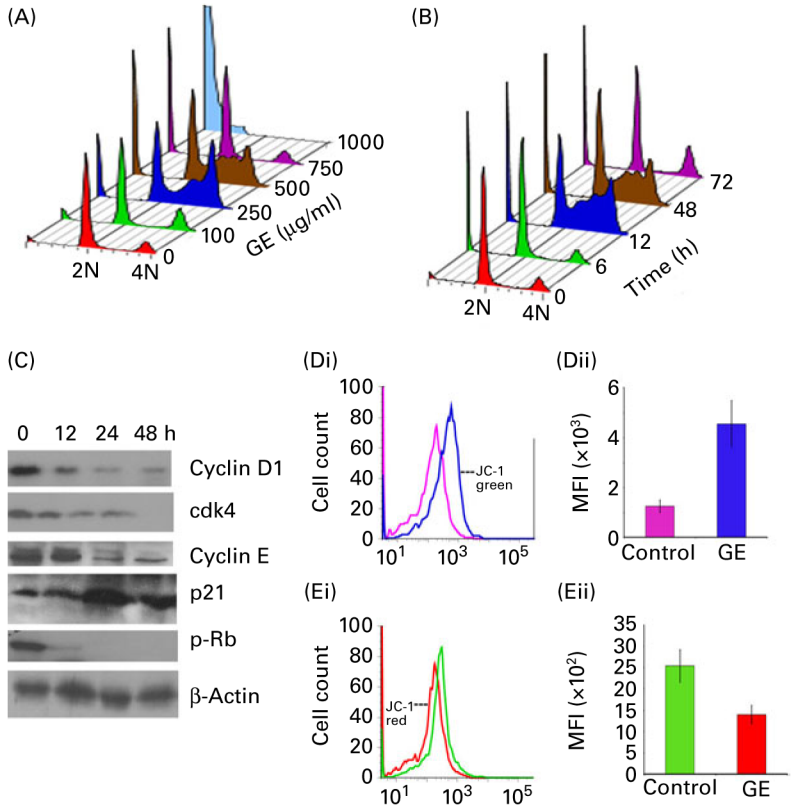

Fig. 2.

Ginger extract (GE) affects cell-cycle progression kinetics by causing the S and G2/M arrest followed by an increase in sub-G1 cell population, suggesting apoptosis. Cell-cycle progression over (A) dose (0–1000 μg/ml) and (B) time (0–72 h) are depicted in a three-dimensional format. Cell populations in G0/G1 appear as 2N (unduplicated) DNA content and G2/M populations are indicated by 4N (duplicated) DNA content. (C) Immunoblots of cell lysates treated in the absence or presence of 250 μg/ml of GE for cyclin D1, cdk4, cyclin E, p21 and p-Rb. Uniform loading was confirmed by β-actin. (Di) Flow cytometric histogram profiles showing percentage of cells with cytosolic monomeric JC-1-associated green fluorescence (indicating collapse of mitochondrial membrane potential) in PC-3 cultures treated with dimethyl sulfoxide (DMSO; control, pink profile; ■) or GE (blue profile; ■) for 24 h. Representative data from a single experiment are shown. (Dii) Quantification of the increase in mean fluorescence intensity (MFI, i.e. the percentage of green JC-1-stained cells) in PC-3 cultures treated with DMSO (control) or GE for 24 h. (Ei) Histogram profiles showing a spectral shift and loss of red fluorescence, consistent with the loss of transmembrane potential on GE treatment (control, green; GE, red). (Eii) Quantification of the decrease in mean fluorescence intensity (i.e. the percentage of red JC-1-stained cells) in PC-3 cultures treated with DMSO (control) or GE for 24 h. Values are means of three independent experiments performed in triplicate, with standard deviations represented by vertical bars ($P < 0{\cdot}05$). (A colour version of this figure can be found online at www.journals.cambridge.org/bjn).

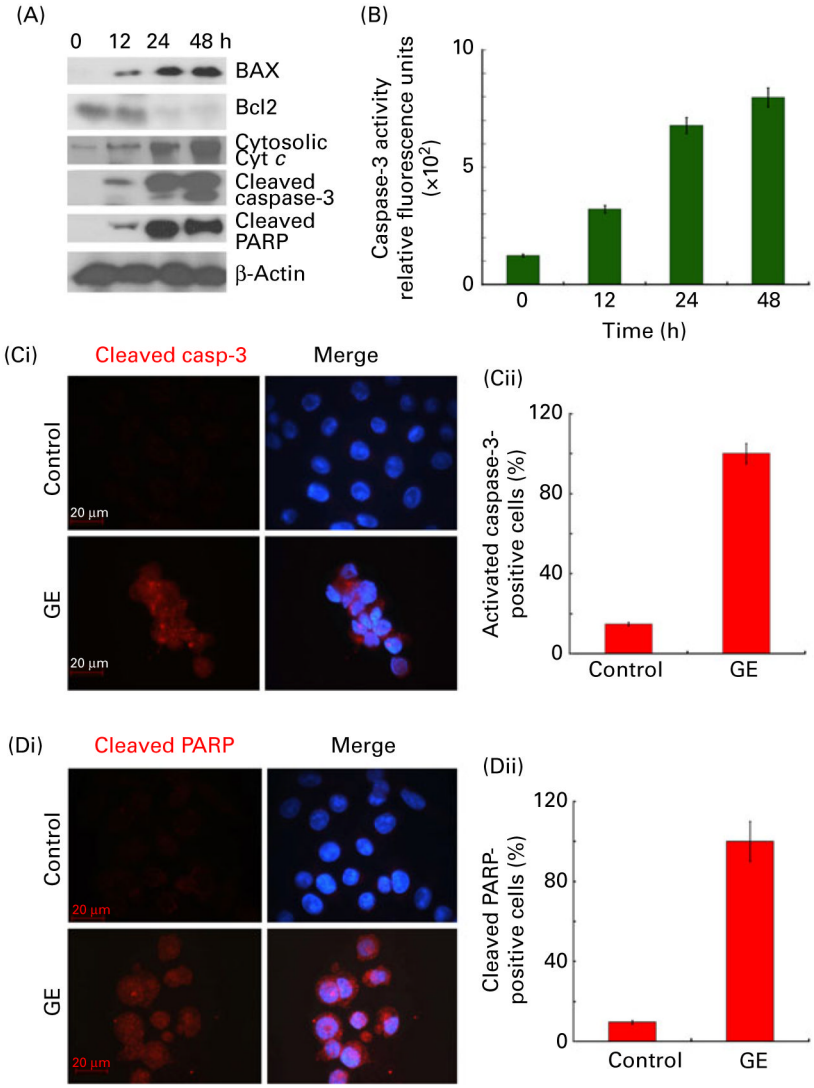

Fig. 3.

Ginger extract (GE) induces mitochondrially mediated intrinsic apoptosis. (A) Immunoblot analyses for BAX, Bcl2, cytoplasmic cytochrome *c* (Cyt *c*), cleaved caspase-3 and poly(ADP-ribose)polymerase (PARP). β-Actin was used as a loading control. (B) Quantification of the time-dependent increase in caspase-3 (Casp-3) activity on GE treatment. Cells were treated with GE for 0, 12, 24 and 48 h, and caspase-3 activity was analysed using the fluorogenic substrate Ac-DEVD-7-amino-4-trifluoromethyl-coumarin. Values are means of three independent experiments performed in triplicate, with standard deviations represented by vertical bars ($P<0{\cdot}05$). Immunofluoresence micrographs of control and 250 μg/ml of GE-treated cells stained for cleaved (Ci) caspase-3 and (Di) PARP. (Cii, Dii) Quantification of activated caspase-3-positive and cleaved PARP-positive cells. (A colour version of this figure can be found online at www.journals.cambridge.org/bjn).

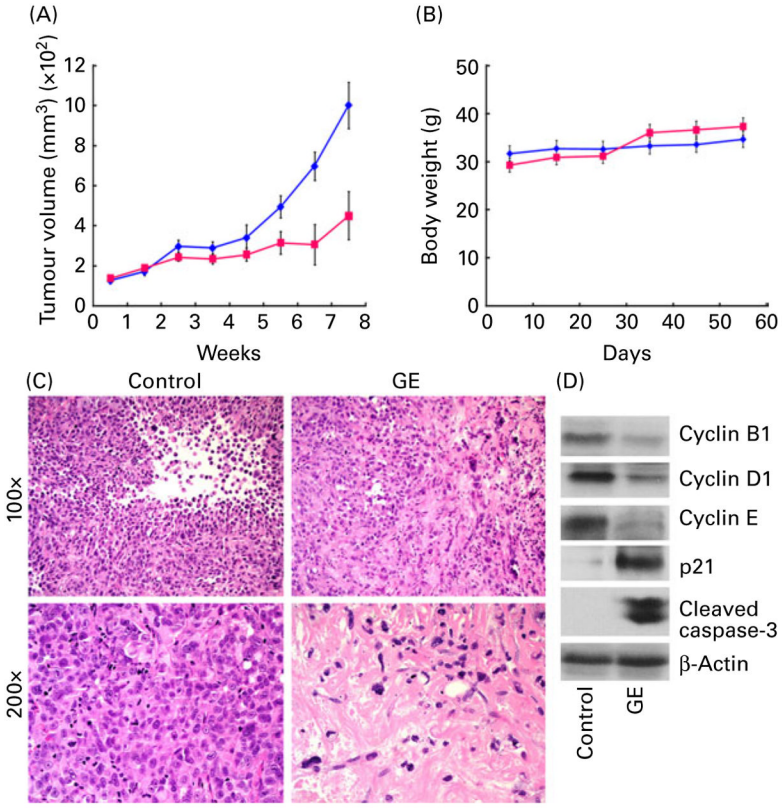

Fig. 4.

Ginger extract (GE) caused *in vivo* inhibition of tumour growth in human PC-3 xenografts on dietary feeding of GE. (A) Progression profile of tumour growth in control vehicle-treated ( ) and GE-treated ( ) mice at the time of treatment. (B) GE treatment was well tolerated, and the body weights of the control ( ) and GE-treated ( ) groups were comparable. Values are means, with standard deviations represented by vertical bars ($n = 6$, $P < 0{\cdot}05$). (C) Tumour micrographs from control and GE-treated mice, respectively, at 100× and 200× magnification. GE-treated tumour microsections reveal large areas of tumour cell death, consistent with the therapeutic effects of GE. Microsections from control tumour tissue show sheets of tumour cells with high-grade pleomorphic nuclei with minimal cell death. (D) Western blot analysis of tumour tissue lysates from control and GE-treated mice for cyclin B, cyclin D1, cyclin E, p21 and cleaved caspase-3. (A colour version of this figure can be found online at www.journals.cambridge.org/bjn).

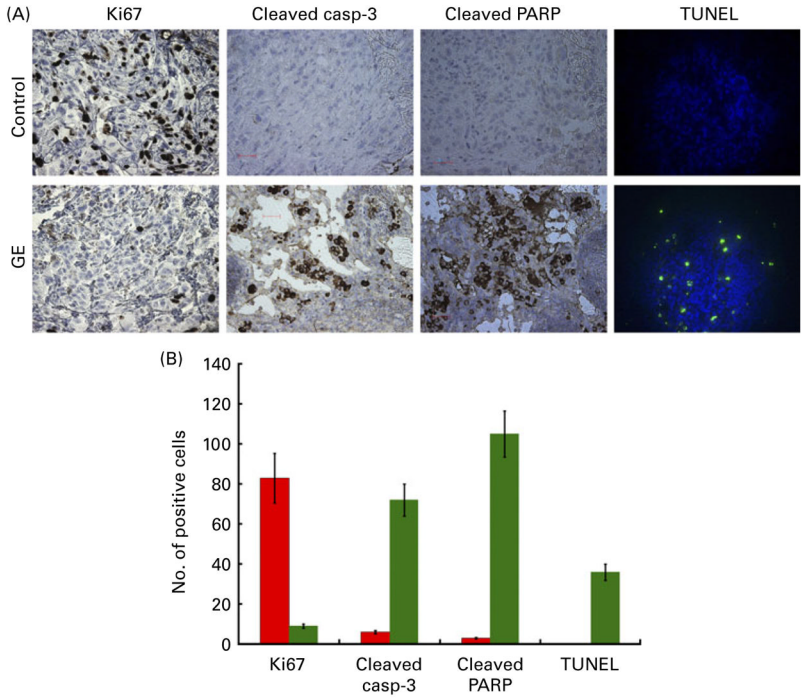

Fig. 5.

(A) Immunohistochemical staining of paraffin-embedded tumour tissue sections from the control and ginger extract (GE)-treated groups for proliferation marker (Ki67) and apoptotic markers (cleaved caspase-3 (casp-3), cleaved poly(ADP-ribose)polymerase (PARP) and terminal deoxynucleotidyl transferase dUTP nick-end labelling (TUNEL)). (B) Quantification of Ki67, cleaved casp-3, cleaved PARP and TUNEL-positive cells counted from several randomly selected fields for a total of 200 cells. Values are means, with standard deviations represented by vertical bars ($P < 0{\cdot}05$). Control, ■; GE, ■. (A colour version of this figure can be found online at www.journals.cambridge.org/bjn).